Piled Raft Foundation with Grid-form Deep Mixing Walls Supporting the Largest Scale Base-isolated Building in Japan

J. Hamada[1], Y. Yamashita[1], T. Honda[1], M. Sugaya[2], M. Kamimura[2]
[1]*Takenaka Research and Development Institute, Takenaka Corporation, Chiba, Japan*
[2]*Building Design Department, Tokyo Main Office, Takenaka Corporation, Tokyo, Japan*
Email: hamada.junji@takenaka.co.jp

ABSTRACT: This paper offers a case history of a piled raft foundation with grid-form deep mixing walls (DMWs) supporting a 10-story base-isolated building of the world's largest scale, measuring 340 m by 180 m in plan. The DMWs play the role of coping with liquefiable sand as well as of reducing settlement of soft cohesive stratum below the sand. Field monitoring of the settlement and the load sharing was performed for over seven years since the beginning of the construction in order to validate the foundation design. The measured settlement of the raft was 10 mm and the ratio of the load carried by piles to the effective structure load was 0.66 at 72 months after the end of construction. In addition to the long term monitoring, seismic measurements of the foundation were performed after the end of the construction. The incremental strain acts on piles, contact earth pressure between raft and soil or DMWs, water pressure beneath the raft and settlements under ground surface were measured during several earthquakes. These values roughly agreed with the design values. Consequently, it is confirmed that a piled raft combined with DMWs works effectively in liquefiable and soft ground.

KEYWORDS: Piled Raft Foundation, Ground Improvement, Load Sharing, Settlement, Seismic Observation, Base Isolated Building.

1 INTRODUCTION

Piled raft foundation is recognized to be a considerable economical foundation system to control settlement of the foundation to an acceptable level without compromising the safety and performance of the foundation by using settlement reducer of piles. Recently, piled raft foundations have been used in many countries, and the settlement and the load sharing between piles and a raft have been carefully investigated for selected structures (Poulos, 2001, Katzenbach et al., 2000, Yamashita et al., 2011).

The piled raft foundations usually can be applied to relatively stiff clays or dense sands, not to soft clays which have a possibility of consolidation settlement or liquefiable loose sands in the condition of ground beneath the raft. Recently, the piled rafts were applied to very soft ground or liquefiable ground by improving subsoil beneath the raft to provide significant load capacity and prevent liquefaction. We developed an advanced type of piled raft combined with grid-form cement deep mixing walls (DMWs) for application to real buildings, and measured the settlements and load sharing (Yamashita et al., 2012; Yamashita et al., 2013; Yamashita et al., 2016).

Furthermore, it is important and necessary to develop more reliable seismic design methods for piled raft foundations, especially in highly active seismic areas. Shaking table tests and static lateral loading tests using centrifuge model or large scale model and analytical studies have been carried out. Mendoza et al. (2000) reported on the static and seismic behaviour of a piled-box foundation supporting an urban bridge in Mexico City clay. Recently, Yamashita et al. (2012) and Hamada et al. (2012) had successfully recorded seismic responses of piled raft foundation supporting a base-isolated building during the 2011 off the Pacific coast of Tohoku Earthquake. These papers show the measured axial force and bending moment of the piles, earth pressure and pore-water pressure beneath the raft, and accelerations of the ground and the structure during the earthquake in which peak ground surface acceleration was 1.75 m/s^2. The results show a decrease in the input motion, which was reduced by the ground improvement, and an increase in bending moments due to horizontal ground deformation. Hamada et al. 2015(a) conducted seismic observations for piled raft foundtion subjected to unsymmetrical earth pressure from just after the 2011 off the Pacific coast of Tohoku Earthquake. However, only a few case histories exist on the monitoring of the soil-pile-structure interaction behavior during earthquakes.

This paper offers a case history of statically monitored settlements and load sharing and seismic observation results of a piled raft with DMWs supporting a 10-story base-isolated building of the world's largest scale, measuring 340 m by 180 m in plan. The

Photo 1 View of monitored building.

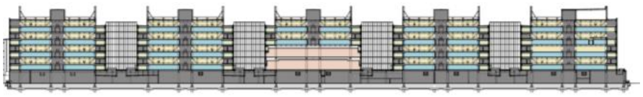

Figure 1 Profile of monitored building.

statically monitored records of the building have been reported by Hamada et al. (2017). In addition to the results, this paper added further long-term results and seismic observation records.

The seismic observation results include during a seismic event on a magnitude of M8.1 at May 30, 2015, Ogasawara event. Accelerations of the building, dynamic sectional forces of the piles and dynamic earth pressure between raft and soil or DMWs were observed. The maximum acceleration of 0.2934 m/s^2 was observed at the base-isolated Pit of the building during the Ogasawara event.

2 BUILDING AND SOIL CONDITIONS

Photo 1 and Figure 1 show a bird's-eye view and a side view of the monitored building. The building is a research institute laboratory for five linked blocks on large-scale artificial ground of base-isolated steel-frame structure, 10 story above the ground–with a 2-story penthouse (the total height is 41.7 m), 340 m by 180 m in plan located in Fujisawa City, Kanagawa Prefecture in Japan. A schematic view of one block with a representive soil profile is shown in Figure 2.

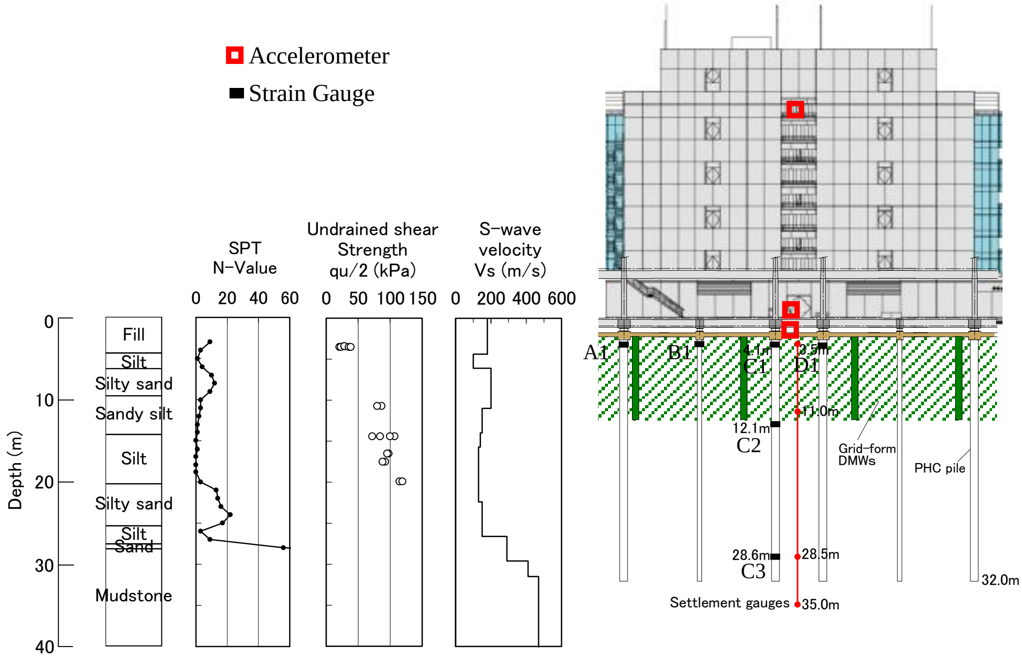

Figure 2 Superstructure and foundation with soil profile.

The subsoil consists of a fill, an alluvial strata of silt and silty sand to a depth of 10 m. Between depths of 10 to approximately 27 m below the ground surface, there lies a silt stratum. It is slightly overconsolidated with an overconsolidation ratio (OCR) of about 1.5. Below the layer, there lies a Pleistocene mudstone of the Kazusa layer. The Kazusa layer appears at a shallow depth in the northwest area of the building site. It is 11 m deep at the shallowest area.

3 FOUNDATION DESIGN

3.1 Liquefaction mitigation

The foundation level was at a depth of 3.0 m below the ground surface, and the ground water table appears approximately 2 m below the ground surface. Assessment of the potential for liquefaction during earthquakes was carried out using a simplified method based on N-value and fine fraction content. It indicated that the silty sand from 6 to 10 m had the potential for liquefaction with PGA of 3.5 m/s^2. Therefore, to cope with the liquefiable silty sand and ensure the bearing capacity of the raft, grid-form DMWs were constructed from the foundation level to a depth of 12 m.

Figure 3 shows a layout of piles and grid-form DMWs. The grid-form DMWs were designed using a simple lattice interval estimation method based on N-value, liquefiable sandy layers

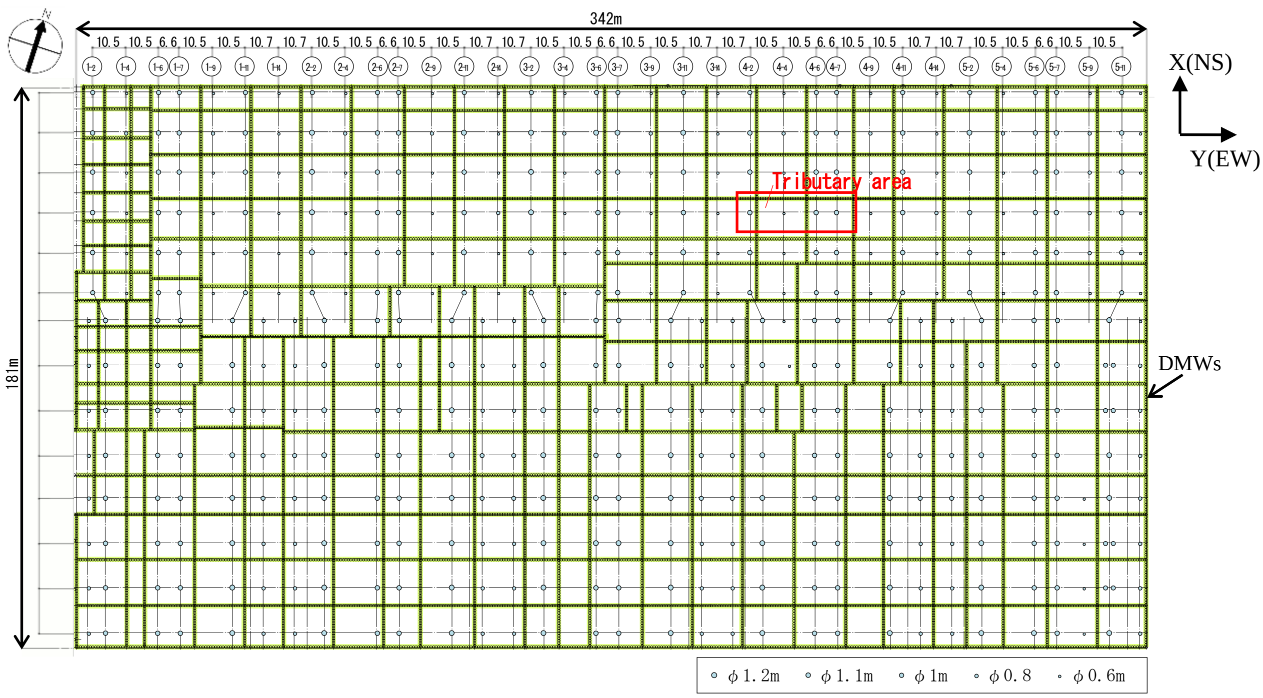

Figure 3 Layout of piles and grid-form deep mixing walls (DMWs).

thickness and its depth (Taya et al., 2008). The compressive strength in designing the soil-cement was 2.0 to 3.0 MPa. The interval between the improved walls (center to center distance of walls) is mainly 15 to 17 m, the ratio of the improved ground area against the original ground area is 0.12. In the northwest area of the building site, where the bearing depth is shallower than that of any other area, the interval between the improved walls is 11 m because of considering the amplified acceleration response of the ground surface.

3.2 Design of piled raft

The total load in the structural design was 4491 MN, which corresponds to the sum of the dead load and live load of the building. The average contact pressure over the raft was 77 kPa. The piled raft foundation was employed to prevent the consolidation settlement of an alluvial silt stratum. Pre-tensioned spun high-strength concrete (PHC) piles (460 pieces in total), mainly ranging from 25 to 29 m (10 to 20 m in northwest area) in length and from 0.6 to 1.2 m in diameter, were used to reduce the settlement and the differential settlement to an acceptable level (see Figure 3). In the foundation design, numerical analysis was carried out to obtain the foundation settlement and load sharing between piles and raft by means of the simplified method of analysis (Yamashita et al. 1998). The foundation maximum settlement was estimated to be 18 mm and load sharing ratio of piles was estimated to be 0.64 in the design.

In the seismic design for the grid-form DMWs, only the longitudinal walls in plane direction were considered to resist the lateral inertial force of the building and the inertial force of soil enclosed by the DMWs, which means that the transverse walls were ignored in terms of resistance elements, judging from a difference in the lateral stiffness. As for the piles, the shear forces and bending moments of piles were estimated in the analytical method, considering the interaction between piles and raft friction (Hamada et al., 2015b). As the aseismic design criteria, the bending moments and shear forces of piles are less than the elastic limit sectional forces against large earthquake motions which recurrence interval is approximately 500 years.

4 INSTRUMENTATION

To confirm the validity of the foundation design, the foundation settlement and the load sharing between piles and raft were measured for the period from the beginning of the construction to 72 months after the end of the construction (E.O.C.). The locations of the monitoring devices are shown in Figure 4.

Four piles (Piles A, C and D with the diameter of 1.1 m, and Pile B with the diameter of 0.6 m) were provided with a couple of LVDT-type strain gauges at a depth of 4.1 m (at the pile heads). In addition to the above depth, the strain gauges were attached to the Pile C at depths of 12.1 m (at the intermediate depth) and 28.6 m (at the pile toe) as shown in Figure. 2. Near the instrumented piles, some earth pressure cells and one piezometer were installed beneath the raft at a depth of 3.0 m. The vertical ground displacements

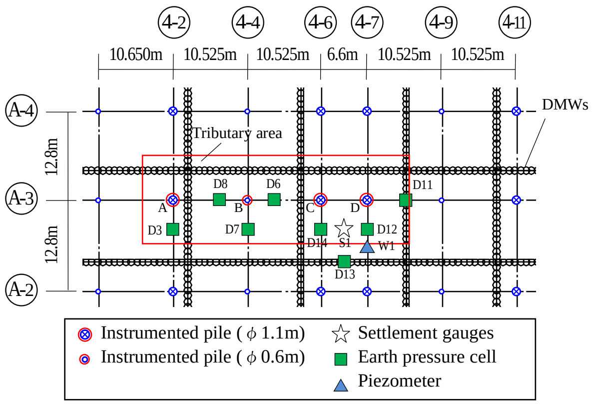

Figure 4 Location of monitoring devices.

below the raft were measured by differential settlement gauges. LVDT-type transducers were installed beneath the raft at depths of 3.5 m, 11.0 m and 28.5 m to measure the relative displacements to a reference point at a depth of 35.0 m of mudstone as shown in Figure 2.

As for the seismic observation, the NS, EW and UD accelerations of the building on the basement floor (Pit), First floor (1F) and Tenth floor (10F) were recorded by triaxial servo accelerometers as shown in Figure 2. The horizontal components of the triaxial accelerometer were oriented to the longitudinal direction, Y(EW) and the transverse direction, X(NS) of the building as shown in Figure 3. The axial forces and the bending moments of four piles, the contact earth pressures between the raft and the soil or DMWs as well as the pore-water pressure beneath the raft were also measured during earthquakes in common starting time with the accelerometers. The triggering acceleration is 0.004 m/s^2 on the Pit and the sampling rate is employed at 100 Hz. Minimum available values of acceleration, strain and earth pressure are 2.4×10^{-4} m/s^2 , 1.0×10^{-4}μ and 5.0×10^{-6} kPa, respectively. Measuring system consists of IC Card Data Logger, Dynamic Amplifier and Power Unit as shown in Table 1.

Table 1 Editorial Instructions

Device	Property
IC Card Data Logger	AD converter 24bit, Sampling 100Hz
Servo Accelerometer	Tri-axis, Full scale:±2000Gal
Dynamic Amplifier	LVDT. Frequency Response:20Hz
Strain gauge	LVDT
Earth pressure cell	LVDT, Capacity:200, 300kPa
Piezometer	LVDT, Capacity:100kPa

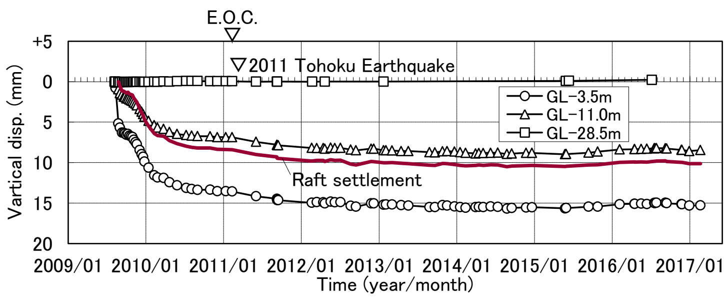

Figure 5 Measured vertical ground displacements below the raft.

5 LONG-TERM STATIC MONITORING

5.1 Settlement

Figure 5 shows the measured vertical ground displacements below the raft. An immediate settlement of 5 mm occurred due to the casting of the 0.6-m-thick foundation slab at GL-3.5 m just below the raft. The red line shows the initialized ground displacement of GL-3.5 m (raft settlement) after casting of the slab. The ground displacement initialized just after the immediate settlement was approximately equal to the settlement of the 'piled raft'. The settlement of the piled raft reached 8.4 mm at the end of the construction and thereafter, slightly increased to 10.0 mm and became stable at 72 months after the E.O.C.

5.2 Pile load and contact pressure of raft

Figure 6 (a) shows the development of the measured axial loads of Piles A, B, C and D. The pile-head loads were 3.8 MN for Pile A, 2.3 MN for Pile B, 4.9 MN for Pile C and 6.2 MN for Pile D at the E.O.C. These loads slightly increased after that and reached 4.9 MN, 3.0MN, 5.9MN and 8.0MN for Piles A, B, C and D, respectively, at 72 months after the E.O.C. These axial loads almost correspond to the design column loads at A, B, C and D of 13.9 MN, 5.5 MN, 12.9 MN and 12.9 MN multiplied by the load sharing ratio of piles, respectively. Figure 6 (b) shows the development of the measured axial loads of Pile C at the (different) depths. The difference between the axial forces at the pile head (GL-4.1 m) and the intermediate depth (GL-12. 1 m) was small because the relative displacement of the pile and ground was small due to the existence of raft and DMWs. The average skin friction around the pile between GL-4.1 m and -12.1 m was 30 kPa at 72 months after the E.O.C. However, the average skin friction between GL-12.1 m and -28.6 m (at the pile toe) was 52 kPa that corresponds to about 60 % of the undrained shear strength of the silt shown in Figure. 2.

Furthermore, the ratio of the axial force at the pile toe to that at the pile head was about 0.35, which was relatively large, compared to previous similar case histories of 0.12 or 0.21 (Yamashita et al., 2012; Yamashita et al., 2013). The following reason was considered for that: Since the pile lengths in this building were shorter than those in the previous case histories (the depth of the pile toe was 50 m below ground surface), and the raft area was larger than in the previous case histories, the skin friction of the piles became relatively small.

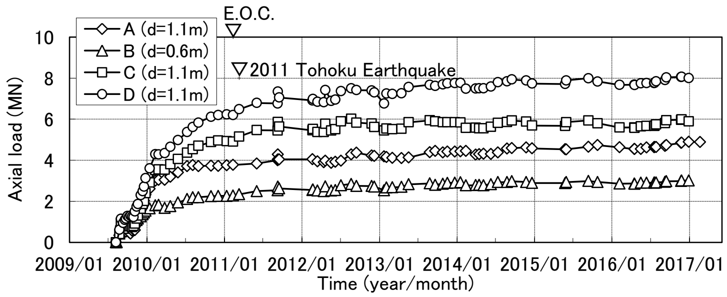

(a) Axial loads at pile head

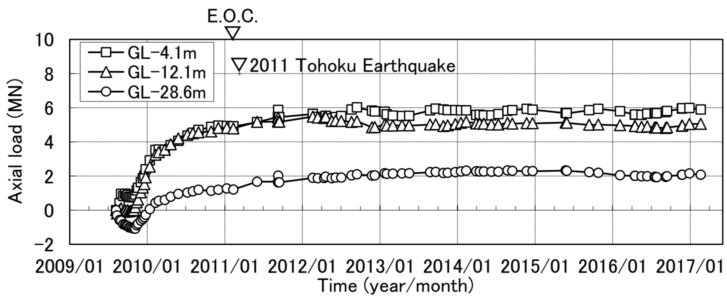

(b) Axial loads of Pile C

Figure 6 Measured axial loads of piles.

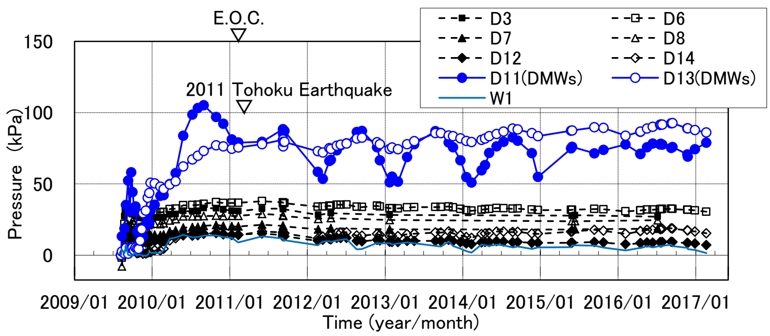

Figure 7 Contact pressures and pore water pressures beneath raft.

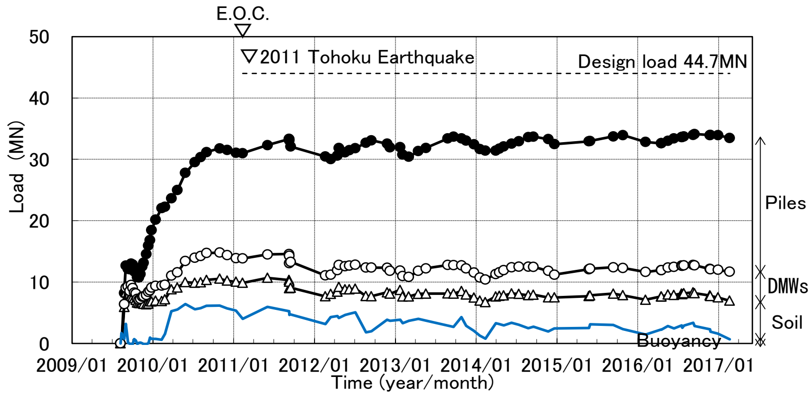

Figure 8 Load sharing between raft and piles in the tributary area vs. time.

Figure 7 shows the development of the measured contact pressures between the raft and the soil, together with the pore-water pressures beneath the raft. The measured contact pressures between the raft and the DMWs (D11 and D13) were larger than those between the raft and the soil as expected. The pressure on D11 shows a seasonal variation. The measured contact pressures at the soil were 7 to 30 kPa, and the pore water pressure was almost 1 kPa, whereas the pressures at the DMWs were 79 to 86 kPa at 72 months after the E.O.C., which were 4 times of those at the soil.

5.3 Load sharing between piles and raft

Figure 8 shows the time-dependent load sharing among the piles, the DMWs, the soil and buoyancy, which are all in the tributary area of Columns A, B, C and D shown in Figure.4. Here, the shared loads carried by the soil were obtained, multiplying the measured contact pressures by the corresponding tributary areas, and the shared loads carried by the DMWs were obtained by averaging the contact pressures of D11 and D13 which were multiplied by the tributary areas of the DMWs respectively. The sum of the measured pile-head loads and the raft load in the tributary area was about 33 MN, which was almost smaller than 44.7 MN, the sum of the four design column loads, but can be almost consistent with the design column loads. The raft load means the sum of the total loads carried by the DMWs and by the soil. It is confirmed that the load carried by the buoyancy was slightly decreasing, whereas the loads carried by the pile heads, the DMWs and the soil were stable after the E.O.C.

The ratios of the loads carried by the piles, the DMWs and the soil to the effective load in the tributary area at 72 months after the E.O.C. were 0.66, 0.14 and 0.19 respectively, where the effective load means the total load minus the buoyancy from the water pressure acting on the base of the raft. These load sharing ratios were almost the same as those in the previous case history using almost the same ratio of the improved area to the DMWs (Yamashita et al., 2013). In the previous case history, the load sharing ratios of the piles, the DMWs and the soil were 0.71, 0.14 and 0.15 respectively. Design load sharing of piles is 0.64, so that the measured value corresponds to the design value.

6. SEISMIC RESPONSE OF STRUCTURE FOUNDATION SYSTEM

6.1 Observed seismic events

Accelerations of the building, dynamic sectional forces of the piles and dynamic earth pressure between raft and soil or DMWs were observed during 74 seismic events from September 15 in 2011 to February 19 in 2017, including an earthquake with a magnitude of M8.1. The maximum acceleration of 0.2934 m/s^2 was observed on the building basement (Pit). Figure 9 shows observed peak accelerations at the basement, Pit. Figure 10 shows a relationship between the peak accelerations at Pit and those at superstructure. The peak accelerations at 1st floor are decreased from that at Pit

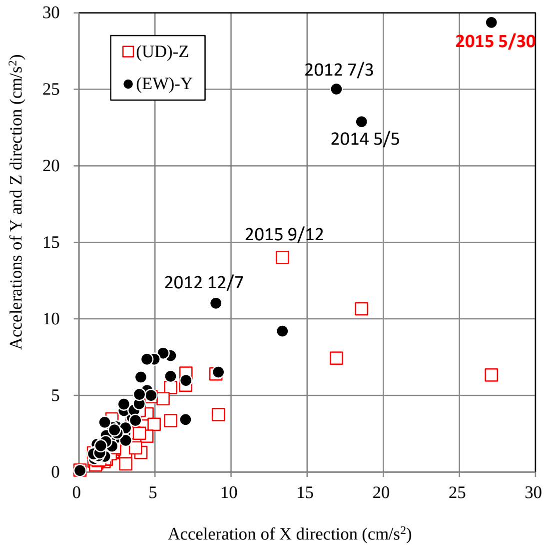

Figure 9 Peak accelerations of seismic events recorded at Pit

within over 10 cm/s^2 due to the base isolation devices. Figure 11 shows the number of the seismic events every month. Figure 12 shows locations of the monitored building and epicenters of large seismic events on May 30, 2015 etc.

6.2 Observed seismic responses of foundation

Figure 13 shows the time histories of the measured accelerations during the seismic event on May 30, 2015. A magnitude of the event is M8.1 and an epicenter of the event is Ogasawara ocean area, in which the maximum acceleration of 0.2934 m/s^2 was recorded in Y-direction (EW).

Figure 14 shows the acceleration response spectrum of the observed accelerations. A natural period of the building estimated by eigen value analysis is about 1.1 sec in the fixed condition of base isolation. The 10th floor was oscillated at a natural period of the building. The domain period of the input earthquake motion at the Pit was from 0.7 sec to 0.8 sec less than the natural period. So, the building will be oscillated at the higher order mode during the earthquake.

Figure 15 shows peak incremental strains on the monitored piles versus peak accelerations during the 74 events. The peak strains mainly occurred by bending moment almost depend on peak accelerations. The strains around pile head at Pile C were smaller than those at intermediate depth and bottom of the pile. It is considered that the strains at the pile head are reduced due to DMWs which can carry the lateral load from the inertial force of superstructure and also can reduce the ground deformation during

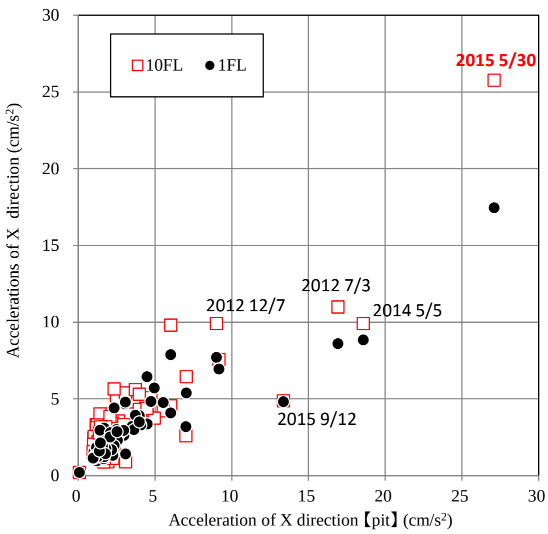

(a) X-direction (NS)

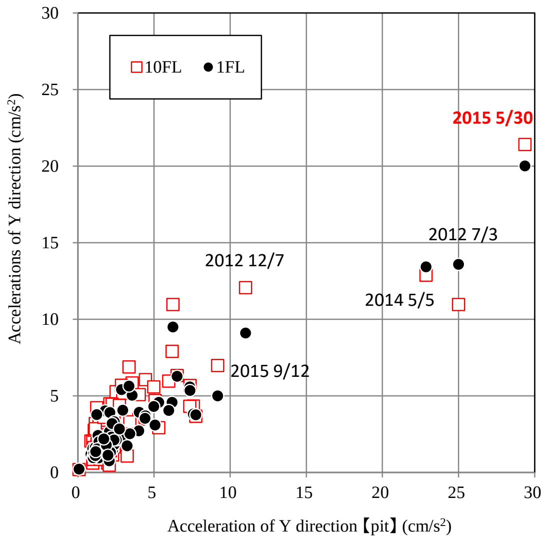

(b) Y-direction (EW)

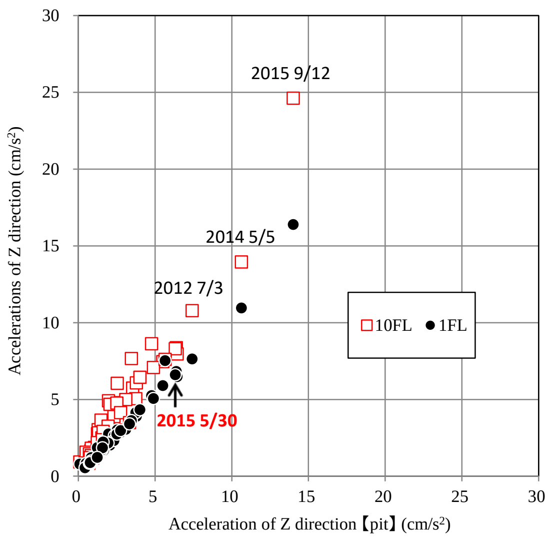

(c) Z-direction (UD)

Figure 10 Relationship between peak accelerations at pit and superstructures

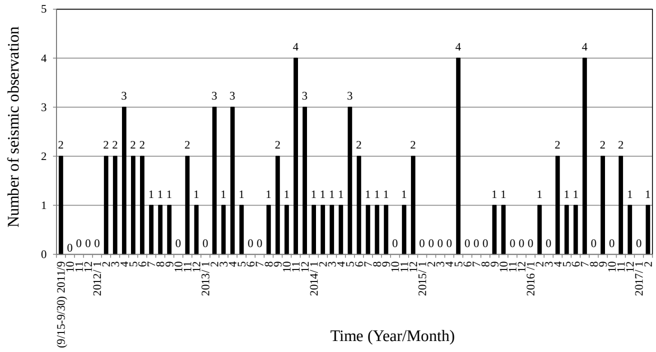

Figure 11 Number of seismic event per month

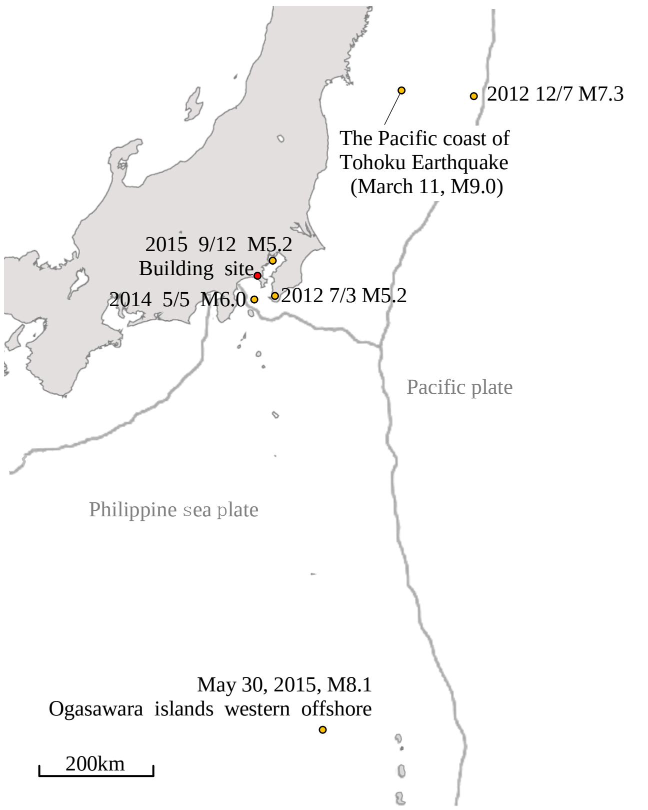

Figure 12 Locations of monitored building and epicenters of seismic events

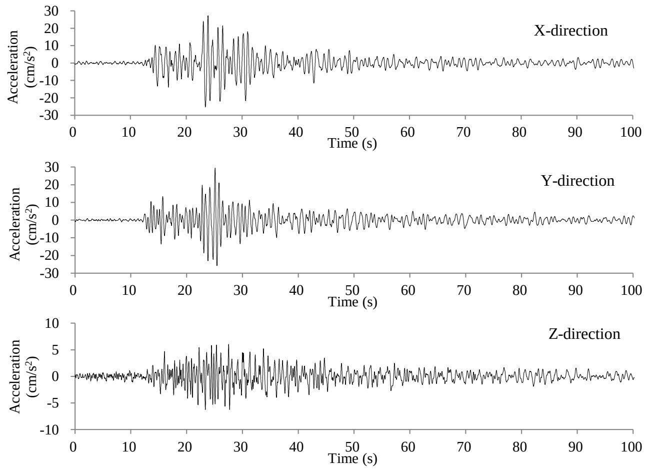

(a) Pit

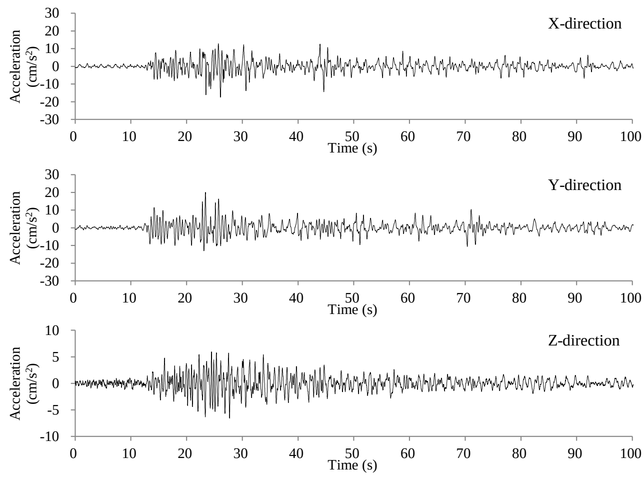

(b) 1st floor

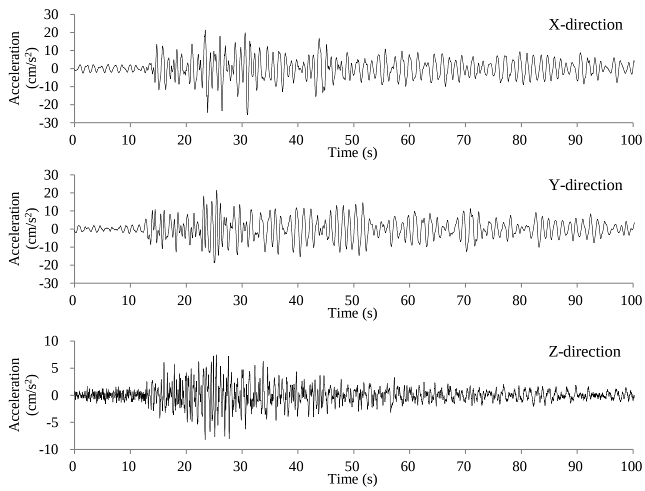

(c) 10th floor

Figure 13 Time histories of the measured accelerations (Ogasawara, May 30, 2015 (M 8.1))

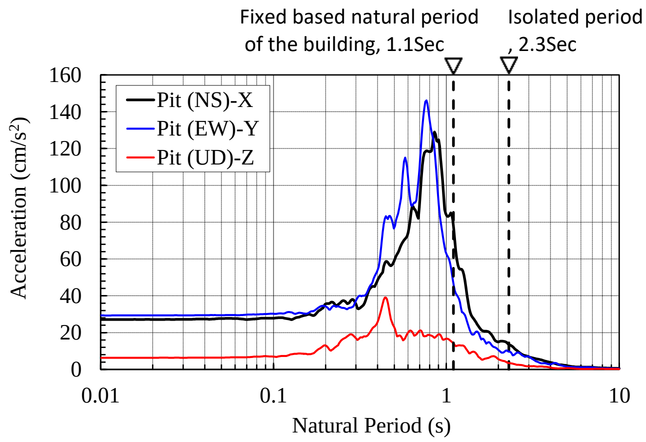

(a) Base isolation Pit

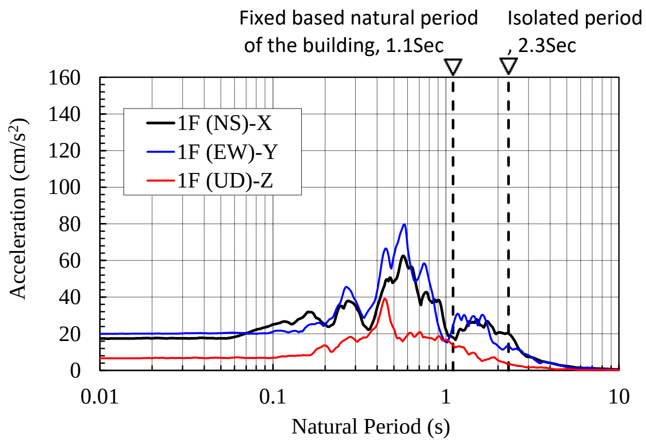

(b) 1st floor

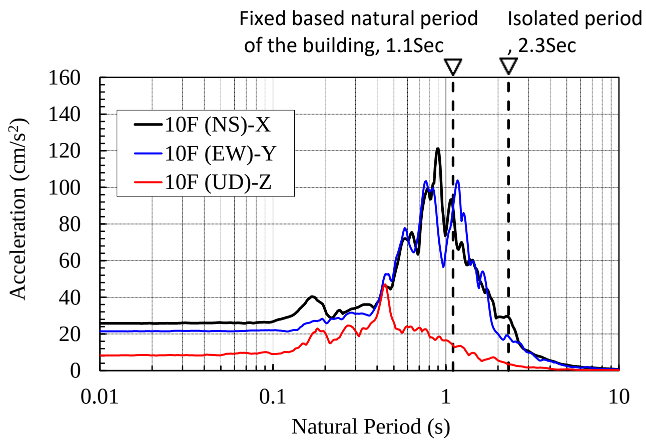

(c) 10th floor

Figure 14 Acceleration response spectrum (Ogasawara, May 30, 2015 (M 8.1))

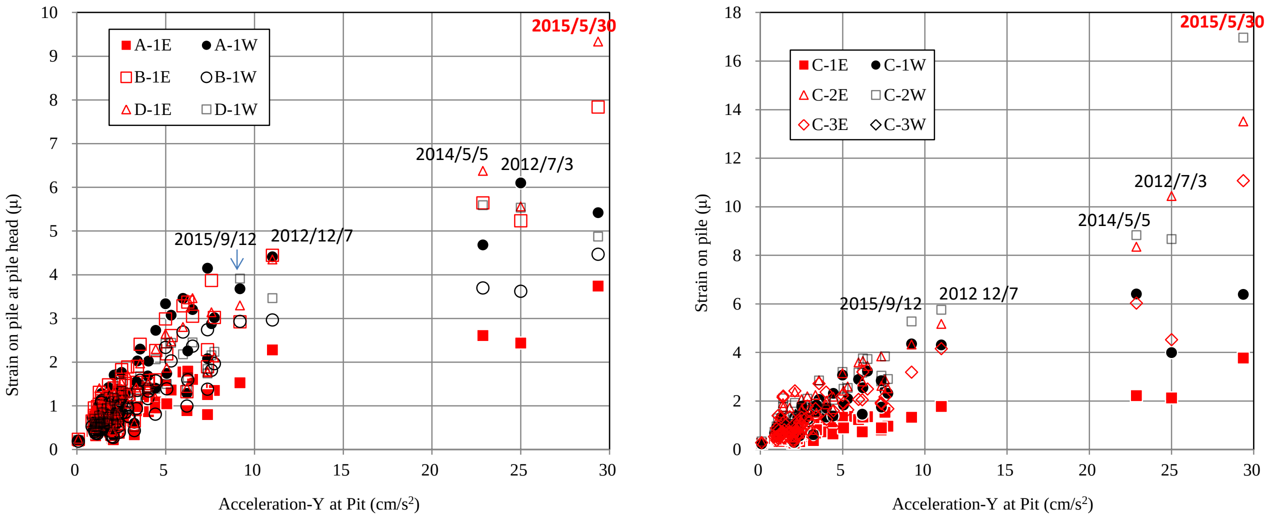

(a) Pile A, B, D (b) Pile C

Figure 15 Peak strain on monitored piles

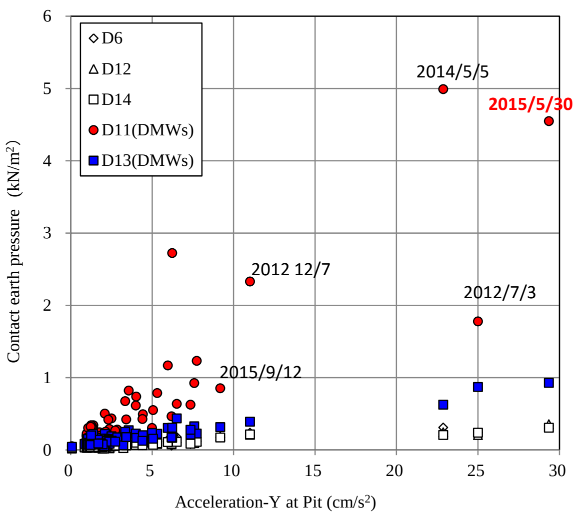

Figure 16 Peak contact earth pressure beneath raft

earthquakes. The peak strain values at intermediate depth near the bottom of DMWs (C-2E, C-2W) are relatively large comparing to those at piled head and pile toe. However the peak value of 17 μ is significantly less than yield strain of 2645 μ.

Figure 16 shows peak contact earth pressure between raft and soil or DMWs. The contact earth pressures on DMWs (D11 and D13) are larger than those on original soil (D6, D12 and D14). This tendency is the same as statically long term monitoring results in Figure 7.

6.3 Effect of 2011 earthquake on settlement and load sharing

On March 11, 2011, one month after the end of the construction, the 2011 off the Pacific coast of Tohoku Earthquake (M_w=9.0) hit the site. The peak horizontal ground acceleration of 0.65 m/s^2 was recorded in K-NET Fujisawa seismic station (NIED online) where is located about 2 km west of the building. No significant change was observed after the earthquake either in the foundation settelement or in the piles-raft load sharing.

7 CONCLUSION

Field monitoring of a piled raft foundation with grid-form cement deep mixing walls supporting a base-isolated building of the world's largest scale has been carried out.

As the result, it was found that the foundation settlement was 10 mm and the ratio of the load carried by the piles to the effective load in the tributary area was estimated to be 0.66 at 72 months after the end of the construction. The grid-form cement deep mixing walls carried 14% of the total load. The DMWs played the role not only of coping with liquefiable sand but also of carrying partial load of the building and thus reducing the settlement of the soft cohesive stratum below the sand.

Seismic observations on the foundation were performed after the 2011 off the Pacific Coast of Tohoku Earthquake. Based on the seismic records, it was confirmed that a lateral inertial force of the building was supported by DMWs and subsoil beneath the raft as well as shear forces of piles judging from observed small strains on piles.

Peak incremental strains on pile heads were smaller than those at intermediate depth and bottom of the pile. It is considered that the strains at the pile head are reduced due to DMWs. The DMWs works well to carry the lateral load from superstructure and also can reduce the ground deformation during earthquake. The peak strain values at intermediate depth near end of DMWs are relatively large comparing to those at piled head and pile toe. However the values are considerably small.

During the monitoring period, the 2011 off the Pacific coast of Tohoku Earthquake struck the site. Almost no change was observed in the settlement or in the load sharing after the earthquake. Consequently, it is confirmed that a piled raft combined with DMWs works effectively in liquefiable and soft ground.

8 REFERENCES

Hamada, J., T., Tanikawa, T., Onimaru, S. and Yamashita, K. (2012) "Seismic observations on piled raft foundation with ground improvement supporting a base-isolated building", Proc. of the 15th WCEE.

Hamada, J., Aso, N., Hanai, A. and Yamashita, K. (2015a) "Seismic performance of piled raft subjected to unsymmetrical earth pressure based on seismic observation records", Proc. of the 6th ICEGE.

Hamada J., Tsuchiya T., Tanikawa T. and Yamashita K. (2015b) "Lateral loading tests on piled rafts and simplified method to evaluate sectional forces of piles", Geotechnical Engineering Journal of the SEAGS & AGSSEA, Vol. 46(2), pp. 29-42.

Hamada, J. and Honda, T. (2017) "Performance of piled raft with grid-form DMWs supporting base-isolated building of the largest scale", Proc. of the 19 th ICSMGE.

Katzenbach R., Arslan U. and Moormann C. (2000) "Piled raft foundation projects in Germany, Design applications of raft foundations", Hemsley J.A. Editor, Thomas Telford, pp. 323-392.

Mendoza, M. J., Romo, M.P., Orozco, M. and Dominguez, L. (2000) "Static and seismic behavior of a friction pile-box foundation in Mexico City clay", Soils & Foundations, Vol.40, No.4, pp. 143-154.

National Research Institute for Earth Science and Disaster Prevention (NIED): K-NET, <http://www.k-net.bosai.go.jp/>.

Poulos H.G. (2001) "Piled raft foundations: design and applications", Geotechnique 51(2), pp. 95-113.

Taya Y., Uchida A., Yoshizawa M., Onimaru S., Yamashita K. and Tsukuni S. (2008) "Simple method for determining lattice intervals in grid-form ground improvement", Japanese Geotechnical Journal, Vol.3(3), pp. 203-212 (in Japanese).

Yamashita K., Yamada, T. and Kakurai, M. (1998) "Simplefied method for analyzing piled raft foundations", Proc. of the 3rd Int. Geotechnical Seminar on Deep Foundations on Bored and Auger Piles, pp. 457-464.

Yamashita K., Yamada T. and Hamada J. (2011) "Investigation of settlement and load shearing on piled rafts by monitoring full-scale structures", Soils & Foundations, Vol.51(3), pp. 513-532.

Yamashita, K., Hamada, J., Onimaru, S. and Higashino, M. (2012) "Seismic behavior of piled raft with ground improvement supporting a base-isolated building on soft ground in Tokyo", Soils & Foundations, Special Issue on Geotechnical Aspects of the 2011 off the Pacific Coast of Tohoku Earthquake, Vol.52, No.5, pp. 1000-1015.

Yamashita K., Wakai S. and Hamada J. (2013) "Large-scale piled raft with grid-form deep mixing walls on soft ground", Proc. of the 18th Int. Conf. on Soil Mechanics and Geotechnical Engineering, 2637-2640.

Yamashita K., Hamada J. and Tanikawa T. (2016) "Static and seismic performance of friction piled raft combined with grid-form deep mixing walls in soft ground", Soils & Foundations, Vol.56(3), pp. 559-573.